Journal of Medicinal and Nanomaterials Chemistry

Orginal Research Article

Electrochemical deposition of tin doped zinc selenide (SnZnSe) thin film material

Imosobomeh Lucky Ikhioya[a,b,c,*] [iD], Donald N. Okoli[c], Azibuike J. Ekpunobi[c]

[a] *Nano Research Laboratory, University of Nigeria, Department of Physics and Astronomy, Nsukka, Enugu State, Nigeria*

[b] *Department of Physics and Astronomy, Faculty of Physical Sciences, University of Nigeria, Nsukka, Enugu State*

[c] *Department of Physics and Industrial Physics, Faculty of Physical Sciences, Nnamdi Azikiwe University, Awka, Anambra State*
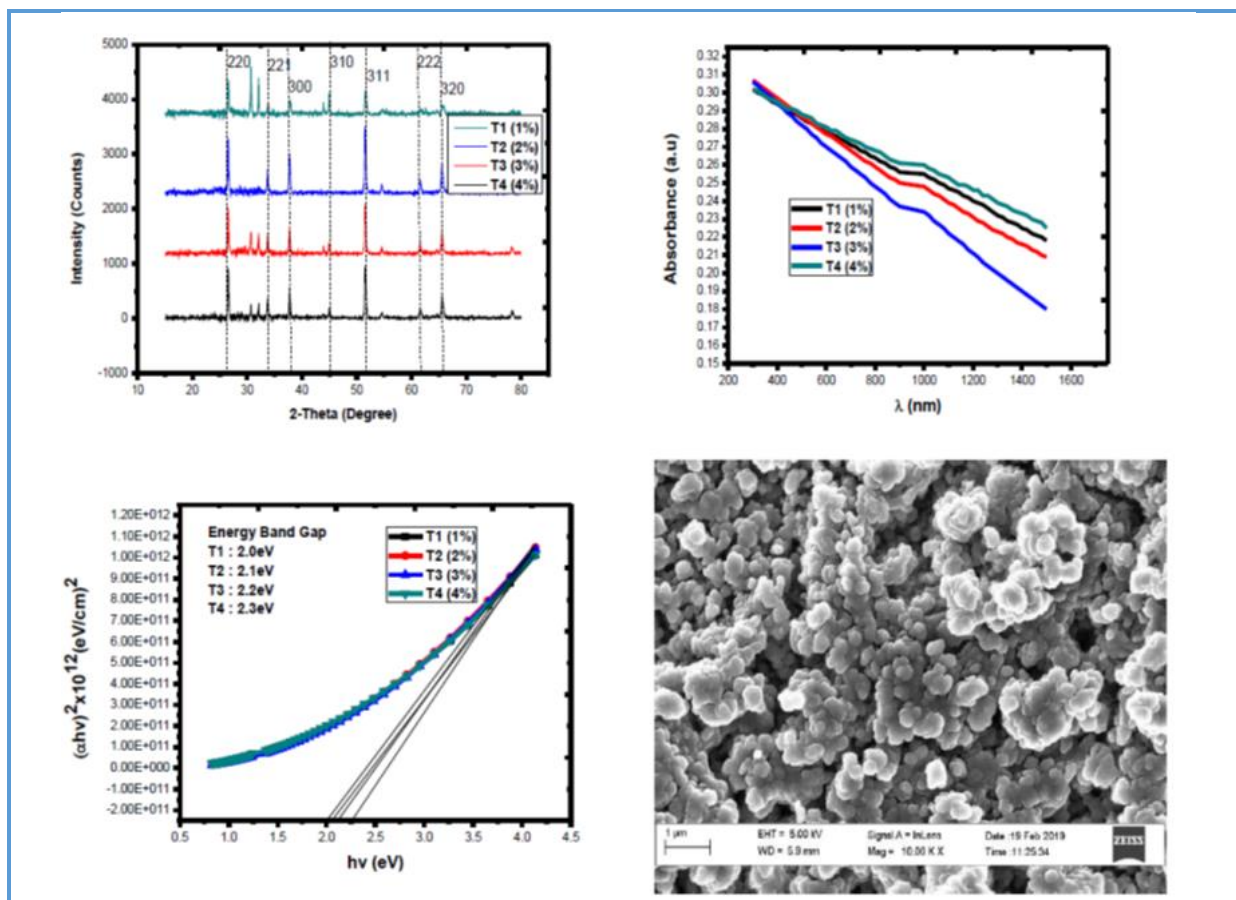
ARTICLE INFORMATION

ABSTRACT

In this research study, the growth of SnZnSe thin film materials was carried out using the cationic precursor, which was an aqueous solution of 0.035 mol solution of $ZnSO_4.7H_2O$ while the anionic precursor was 0.1 mol solution of selenium metal powder was prepared by dissolving with 4 mL of hydrogen chloride (HCl). The XRD of the films deposited on FTO substrates at different dopant concentration 1%, 2%, 3% and 4% showed the reflection peaks at (220), (221), (300), (310), (311), (222) and (320) with the lattice constant of a=7.189 Å. The SEM results revealed the random distribution of tiny nano-grains on the substrate, the nano-grains were observed to agglomerate due to the presence of large free energy characteristics of small particles. The optical bandgap of the deposited material enhanced from 2.0-2.3 eV as the dopant concentration increased.

Corresponding author, email: Imosobomeh.ikhioya@unn.edu.ng (I.L. Ikhioya).
Tel.: +23408038684908.

Graphical Abstract

Introduction

The metal chalcogenides are regarded as a versatile semiconductor in thin-film materials which play an important role in our modern-day electronics, semiconducting materials, including transistors, diodes, integrated circuits, photovoltaic and other solid-state devices [1, 2]. Such devices have found wide applications due to their numerous advantages such as compact sizes, reliability, power efficiency, and low cost [3, 35–37]. As discrete components, they have used in power devices, optical sensors, and light emitters, including solid-state lasers [4]. More importantly, they can be easily incorporated into easily manufacturable microelectronic circuits. They are and will continue to be one key element for

almost all electronic systems in the foreseeable future [5]. Thin films are crystalline or non-crystalline materials developed two-dimensionally on the surface of a substrate by physical or chemical methods. They play a vital role in nearly all electronic and optical devices [6]. They have been used as electroplated films for decoration and protection [7]. They have long been used as anti-reflection coatings on window glass, video screens, camera lenses and other optical devices [8]. These films are more than 100 nm thick, made from dielectric transparent materials and have refractive indices less than that of the substrate [9].

Zn based nanostructures have been widely investigated recently due to its different potential applications [10–12]. Zinc selenide (ZnSe) shows unique optical properties

exhibiting some potential applications, such as blue-green light-emitting diodes, photo-luminescent, and electro-luminescent devices, lasers, thin-film solar cell, nonlinear optical crystal and infrared optical material [13, 14]. ZnSe and its lattice-matched ternary alloys have been regarded as useful II-VI compound semiconductors for optoelectronic and photoelectronic devices. For the energy ranges from visible to ultraviolet, ZnSe based materials are structured the first manifestation of the blue-green laser in 1991 [15–17]. ZnSe has been a material of choice for blue diode lasers and photovoltaic solar cells since its bulk bandgap is 2.7 eV, which can be tuned by adding impurities [11, 18, 19]. Out of varieties of applications, ZnSe can be used as optically controlled switching devices [20, 21]. Therefore, it is of great interest as a model material as a thin film, quantum wells, bulk crystals, and nanodots. Since the last few decades, the nanosized materials have been subject to great interest due to their unique physical and chemical properties. Thus the strong, size-dependent optical emission of many semiconductor nanostructures makes them promising candidates for use as fluorescent tags in the study of biological systems. Over the years, ZnSe thin films have been obtained by serval preparation approaches including sputtering [22, 23], molecular beam epitaxy [24], pulsed laser deposition [25], chemical vapor deposition [26], successive ionic layer adsorption and reaction [27], spray pyrolysis [28], chemical bath deposition (CBD) [22, 29] and electrodeposition [10]. Among these techniques, electrochemical deposition offers several advantages: it is relatively economical; it can be used on a large scale.

In this research, we reported on growth and characterization of SnZnSe via electrochemical deposition technique, to study kind of transitions on the structural, morphological and optical properties and the elemental composition of the deposited material for photovoltaic application.

Experimental

Materials and methods

The chemicals used in this work were analytical grade and purchased from Sigma-Aldrich. The growth of SnZnSe thin-film semiconductor material included zinc tetraoxosulphate (VI) heptahydrate ($ZnSO_4.7H_2O$), Tin chloride ($SnCl_2.2H_2O$), selenium metal powder (Se), and hydrogen chloride (HCl). Electrochemical deposition technique (ECD) was used in this work which involves the deposition of any substance on an electrode as a result of electrolysis which is the occurrence of chemical changes owing to the passage of electric current through an electrolyte. This process involves oriented diffusion of charged growth species through a solution when an external field is applied and reduction of charged growth species at the growth or deposition which also serves as an electrode. The electrochemical bath system is composed of a source of the cation (i.e $SnCl_2.2H_2O$, $ZnSO_4.7H_2O$ for Sn^{2+}, Zn^{2+}), a source of the anion (i.e Selenium metal powder for Se^2), deionized water all in 100 mL beaker, the magnetic stirrer was used to stir the reaction bath. The power supply was used to provide an electric field (DC voltage), a conducting glass was used as the cathode while the anode was carbon and fluorine electrode. Finally, uniform deposition of thin films by electrochemical deposition technique was achieved (Figure 1).

Substrate cleaning procedure

Attention was paid on the cleaning and activating the substrate surface. The selection of the substrate and methods used for the cleaning

of the surface of the substrate are very important in the formation of thin films with a reproducible process. Nature of the material, size, surface roughness and cleanliness of the substrate play a crucial role in formation of the film and its properties such as adhesion, pin-hole density, porosity, film microstructure, morphology, and mechanical properties.
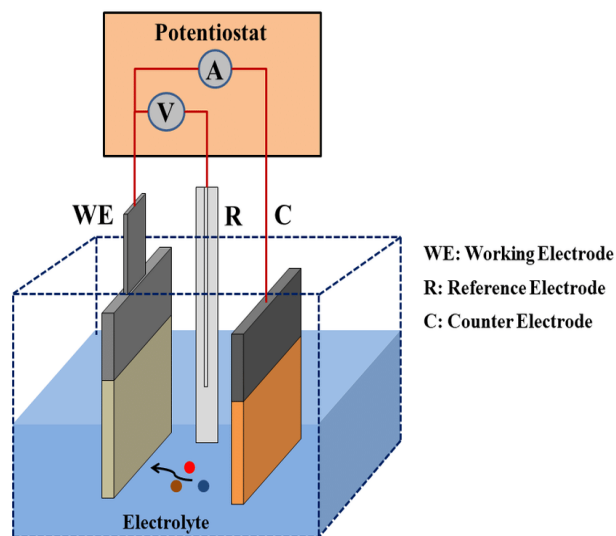

Figure 1. Schematic diagram of electrochemical deposition technique

Substrate cleaning usually involves removing surface contaminations like greasy particles, dust, and metals. The cleaning process varies with the substrate being cleaned. The contaminants present in the surface of the substrate can be broadly categorized into two types, namely organic and inorganic. Organic contaminants can be easily removed by emulsifying the surface of the substrate with washing solutions. However, for the removal of inorganic contaminants, a direct mechanical approach is needed when they are in particle form. Several procedures are available for this purpose such as immersing in solvents, ultrasonic cleaning, and electronic discharge. The systematic procedure used for cleaning the substrates is; transparent fluorine doped tin oxide (FTO) coated glass substrates with a sheet resistance of 10 Ω/m was used as a substrate for deposition.

Growth of SnZnSe thin films

The growth of SnZnSe thin film materials was carried out using the cationic precursor which was an aqueous solution of 0.035 mol solution of $ZnSO_4.7H_2O$ while the anionic precursor was 0.1 mol solution of selenium metal powder was prepared by dissolving with 4 mL of Hydrogen chloride (HCl). This was to ensure uniform deposition. The electrochemical deposition bath system is composed of a source of cation $SnCl_2.2H_2O$, $ZnSO_4.7H_2O$ for Sn^{2+}, Zn^{2+}), a source of the anion (i.e Selenium metal powder for Se^{2-}), distilled water all in 100 mL beaker, and a magnetic stirrer which was used to stir the reaction bath. The power supply was used to provide electric field (DC voltage), a Fluorine doped tin oxide (FTO) was used as the cathode while the anode was carbon and fluorine electrode. The molar concentration of the solution was varied in the process of the experiment (Table 1).

Table 1. Variations of growth materials

Sample	$SnCl_2.2H_2O$ (mL)	$ZnSO_4.7H_2O$ (mL)	Se (mL)	Dopant Conc. (%)	Time (Sec)	Voltage (V)
T1	10	20	20	1%	25	10
T2	10	20	20	2%	25	10
T3	10	20	20	3%	25	10
T4	10	20	20	4%	25	10

Characterization of films

The growth films were characterized for their optical properties, electrical properties, scanning electron microscope, and structural properties.

The structural characterization of the films was carried out using the Bruker D8 Advance X-ray diffractometer with Cu-Kα line (λ=1.54056 Å) in 2θ range from 10°–90° the instrument helped in determining the type of lattice crystal and intensities of diffraction peaks, with the help of database software supplied by the international center of diffraction data.

The quantitative analysis of the films was carried out using energy dispersive X-ray analysis (EDX) for thin films to study the stoichiometry of the film. This unit is attached to the Zeiss scanning electron microscope (SEM).

When a beam of electrons strikes the specimen, some of the incident electrons excite the atom of the specimen which emits X-ray on returning to the ground state. The energy of the X-ray is related to the atomic number of the exciting element. Lithium drifted Si-diode, held at liquid nitrogen temperature is used as a detector of the X-rays. JEOL-JSM 7600F Japan was employed in the present investigation. The electrical characterizations of the films were measured using a four-point probe.

The absorbance spectral of the films was obtained in UV-visible NIR using UV-1800 visible spectrophotometer. UV-visible spectrophotometer uses the principle that when a beam of electromagnetic radiation of initial flux I is incident on a transparent object, it is transmitted. Some parts of the incident flux could be absorbed for an absorbing medium while some parts could be reflected. Various other parameters from the absorbance include: transmittance, reflectance, refractive index, optical thickness, coefficient of absorption, extinction coefficient, optical conductivity, and dielectric constants were derived using the formula below (a) from the law of conservation of energy we obtained,

$$A+T+R=1 \tag{1}$$

Where A is the absorbance, R is the Reflectance, and T is the transmittance.

Results and Discussion

Structural analysis of SnZnSe thin films

The XRD pattern of SnZnSe thin films deposited on FTO substrates at different dopant concentrations 1%, 2%, 3%, and 4% is showed in Figure 2. The diffraction peaks showed at (220), (221), (300), (310), (311), (222) and (320) corresponds to the following angle (26.220), (36.880), (36.890), (51.800), (55.000), (62.700) and (66.000) respectively. SnZnSe thin films are indexed to be face-centred cubic structure of [JCPDS card no. 01-088-2345] reported by [38, 39]. The un-indexed peaks could have possibly resulted from the FTO substrates used for deposition. The lattice constant a=7.189 Å was obtained using (Equation 2). The higher peaks in the plot could result to the increased in film's thickness with an increase in dopant concentration, thus creating a larger surface area for photovoltaic devices and solar cell activities. The average crystallite size of the films was determined using the Debye-Scherer's equation. (Equation 2). Table 2 showed the calculated crystallite or grain sizes and dislocation density for the films deposited at different dopant concentrations 1%, 2%, 3%, and 4%.

$$d=\frac{n\lambda}{2sin\theta} \tag{2}$$

$$D=\frac{0.94\lambda}{\beta Cos\theta} \tag{3}$$

$$K = 2(\frac{In}{\lambda})^{\frac{1}{2}} = 0.94 \tag{4}$$

Where D is the average crystallite size, λ is the wavelength of the X-ray source (0.15416 nm), β is the angular line width at half maximum intensity in radians, and θ is the angle between the incident beam and the scattering plane. The constant of proportionality K is the Scherer constant which depends on how the width is determined, the shape of the crystal and the size distribution. Although the shape of the crystallites is usually irregular, we can often approximate them as spheres, parallelepipeds, prisms or cylinders. The value of the Scherer constant K for spherical crystals and parallelepiped like ours is 0.94 [32]. The value of the Scherrer constant K, was estimated as 0.94 for crystallite size using Equation (4).
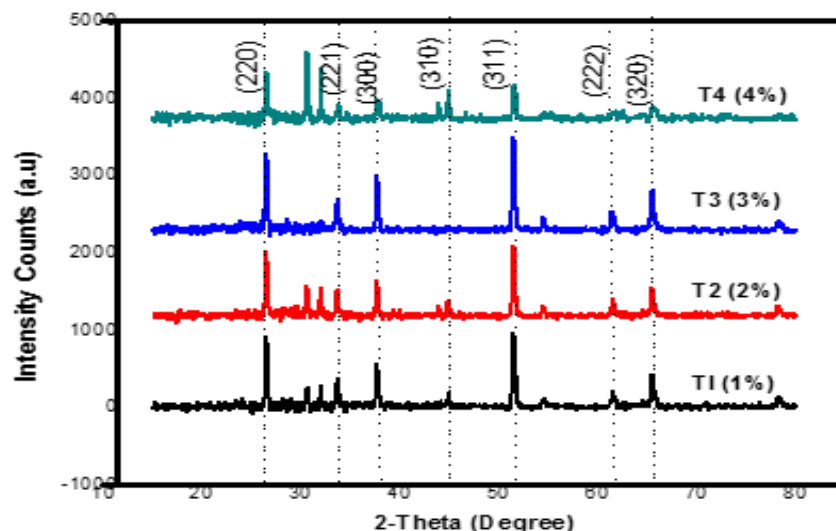

Figure 2. XRD pattern of SnZnSe deposited at different dopant concentration

Table 2. Structural parameters of SnZnSe thin film deposited at different dopant concentration

Sample	2θ (degree)	d (spacing) Å	Lattice constant (Å)	(β) FWHM	(hkl)	Grain Size (D) nm	Dislocation density,σ lines/m²
T1 (1%)	26.22	3.49173	7.189	0.92832	220	1.60172	0.38978
	36.88	2.50386		0.92832	221	1.64410	0.36981
	36.89	2.50320		0.92832	300	1.64445	0.36978
	51.80	1.81317		0.92832	310	1.73416	0.33252
	55.00	1.71521		0.92832	311	1.75869	0.32331
	62.70	1.52230		0.92832	222	1.82666	0.29969
	66.00	1.45417		0.92832	320	1.86006	0.28903
T2 (2%)	26.22	3.49173	7.189	0.91270	220	1.62913	0.37677
	36.88	2.50386		0.91270	221	1.67255	0.35747
	36.89	2.50320		0.91270	300	1.67260	0.35744
	51.80	1.81317		0.91270	310	1.76384	0.32142
	55.00	1.71521		0.91270	311	1.78879	0.31252
	62.70	1.52230		0.91270	222	1.85792	0.28969
	66.00	1.45417		0.91270	320	1.89189	0.27938
T3 (3%)	26.22	3.49173	7.189	0.67700	220	2.19632	0.20730
	36.88	2.50386		0.67700	221	2.25485	0.19668

	36.89	2.50320		0.67700	300	2.25492	0.19666
	51.80	1.81317		0.67700	310	2.37792	0.17684
	55.00	1.71521		0.67700	311	2.41156	0.17194
	62.70	1.52230		0.67700	222	2.50476	0.15939
	66.00	1.45417		0.67700	320	2.55056	0.15371
T4 (4%)	26.22	3.49173	7.189	0.56600	220	2.62705	0.14489
	36.88	2.50386		0.56600	221	2.69706	0.13747
	36.89	2.50320		0.56600	300	2.69714	0.13746
	51.80	1.81317		0.56600	310	2.84427	0.12361
	55.00	1.71521		0.56600	311	2.88450	0.12018
	62.70	1.52230		0.56600	222	2.99598	0.11140
	66.00	1.45417		0.56600	320	3.05076	0.10744

Surface morphological and EDX analysis

The surface morphology of SnZnSe thin film grown on fluorine-doped tin oxide (FTO) substrates at a different dopant concentration of 1%, 2%, 3% and 4%, as shown in Figure 3. It shows the random distribution of tiny nano-grains on the substrate, the nano-grains were observed to agglomerate due to the presence of large free energy characteristics of small particles. As the dopant concentration increases from 1-4% the nano-grain becomes more densely packed. The grown films were homogenous and without cracks [38, 39]. Figure 4 and 5 shows the energy dispersive X-ray spectra of SnZnSe thin film grown at 1% and 5% respectively.
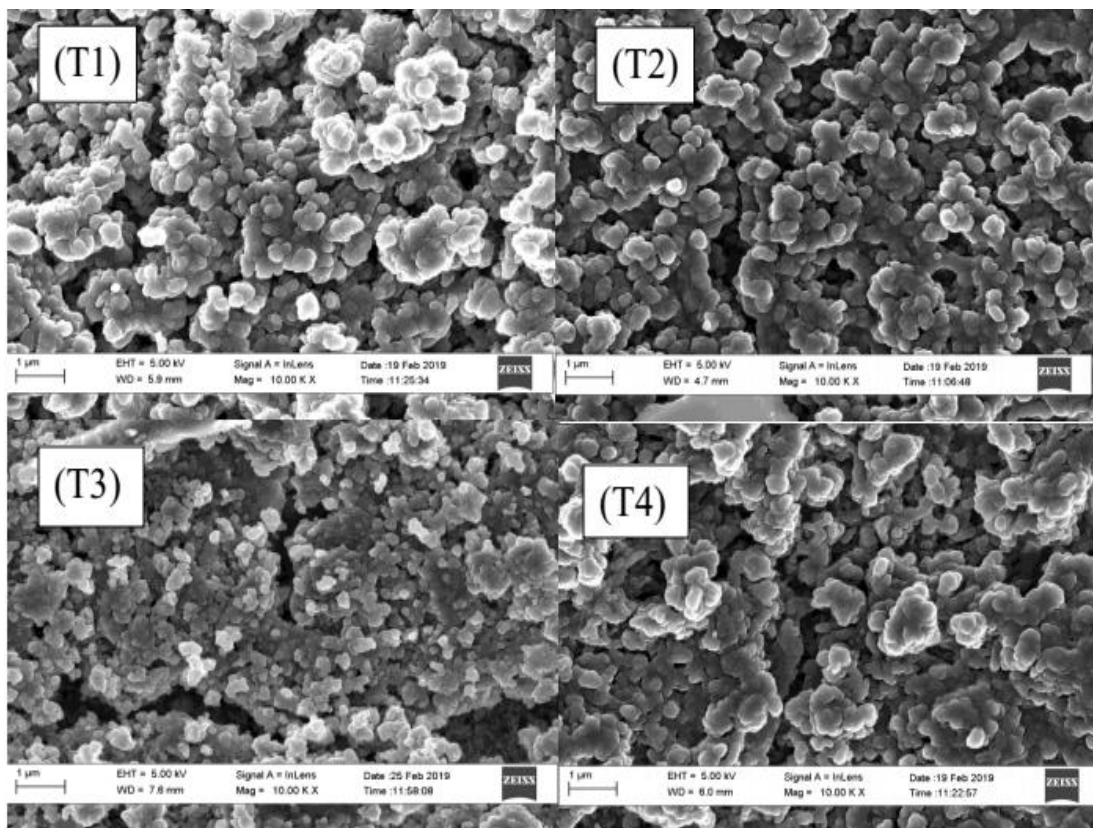

Figure 3. SEM micrograph of SnZnSe film (T1) 1%, (T2) 2%, (T3) 3% and (T4) 4%
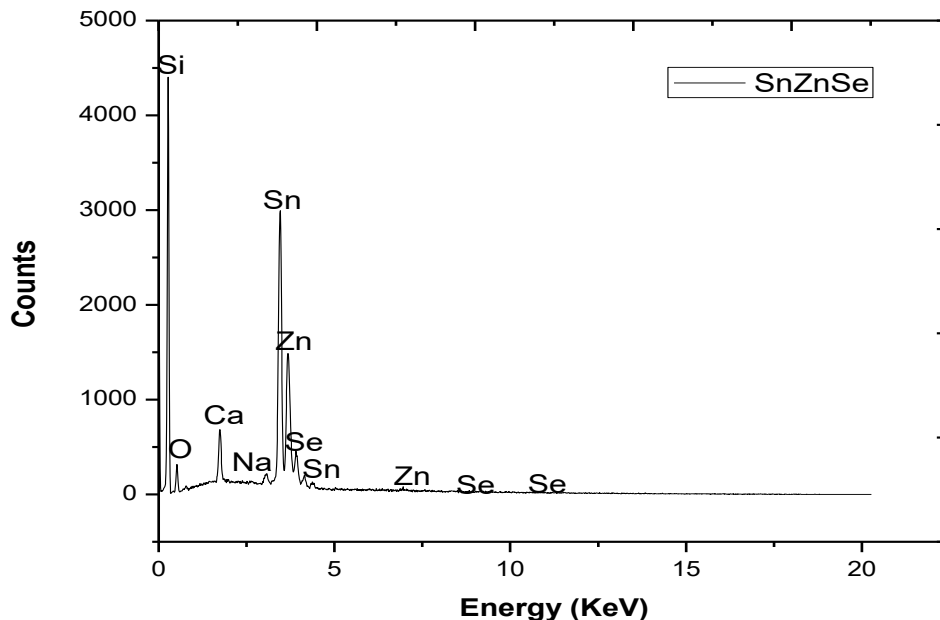
Figure 4. Energy dispersive X-ray spectra (EDX) of SnZnSe

Optical study of tin zinc selenide

The optical absorbance spectra of the SnZnSe thin films grown at varying dopant concentrations of 1%, 2%, 3% and 4% are demonstrated in Figure 5**a**. From the plot sample T1, T2, T3, and T4 revealed that as the wavelength of the incident radiation increase the absorbance of SnZnSe thin films decreases. The material grown at 1% and 4% has the same thread which reveals the lowest and the material is grown at 2% and 3% reveals highest which shows that SnZnSe cells grown will be a good material that will absorb energy from the Sun [38, 39]. SnZnSe cells can also serve as photovoltaic devices and other applications in the electronics industry. It was also noticed that SnZnSe can be used in the mass production of solar cells for the fabrication of lasting solar panels for alternative energy supply.

The optical transmittance spectra of SnZnSe thin films in Figure 5**b** grown under the same parametric conditions and at varying dopant concentration of 1%, 2%, 3% and 4% for sample T1, T2, T3, and T4 reveal that as the wavelength of the incident radiation increase the transmittance of SnZnSe thin films increases. The material grown at 2% and 3% transmit above 60% of the transmittance while the material grown at 1% and 4% transmit above 50% of transmittance which reveals the highest and lowest optical transmittance which shows that SnZnSe cells grown will be a good material that will absorb energy from the sun [38, 39]. SnZnSe cells can also serve as a photovoltaic device and other applications in the electronics industry. It was also noticed that SnZnSe can be used in the mass production of solar cells for the fabrication of lasting solar panels for alternative energy supply.

The optical reflectance of SnZnSe thin films in Figure 5**c** grown under the same parametric conditions and at varying dopant concentration of 1%, 2%, 3% and 4% for sample T1, T2, T3, and T4 reveal that as the wavelength of the

incident radiation increase the reflectance of SnZnSe thin films decreases. The material grown at different dopant concentrations follows the same thread at the infrared region of the spectrum which reveals the highest optical reflectance which shows that SnZnSe cells grown will be a good material that will absorb energy from the sun [38, 39]. SnZnSe cells can also serve as a photovoltaic device and other applications in the electronics industry. It was also noticed that SnZnSe can be used in the mass production of solar cells for the fabrication of lasting solar panels for alternative energy supply.
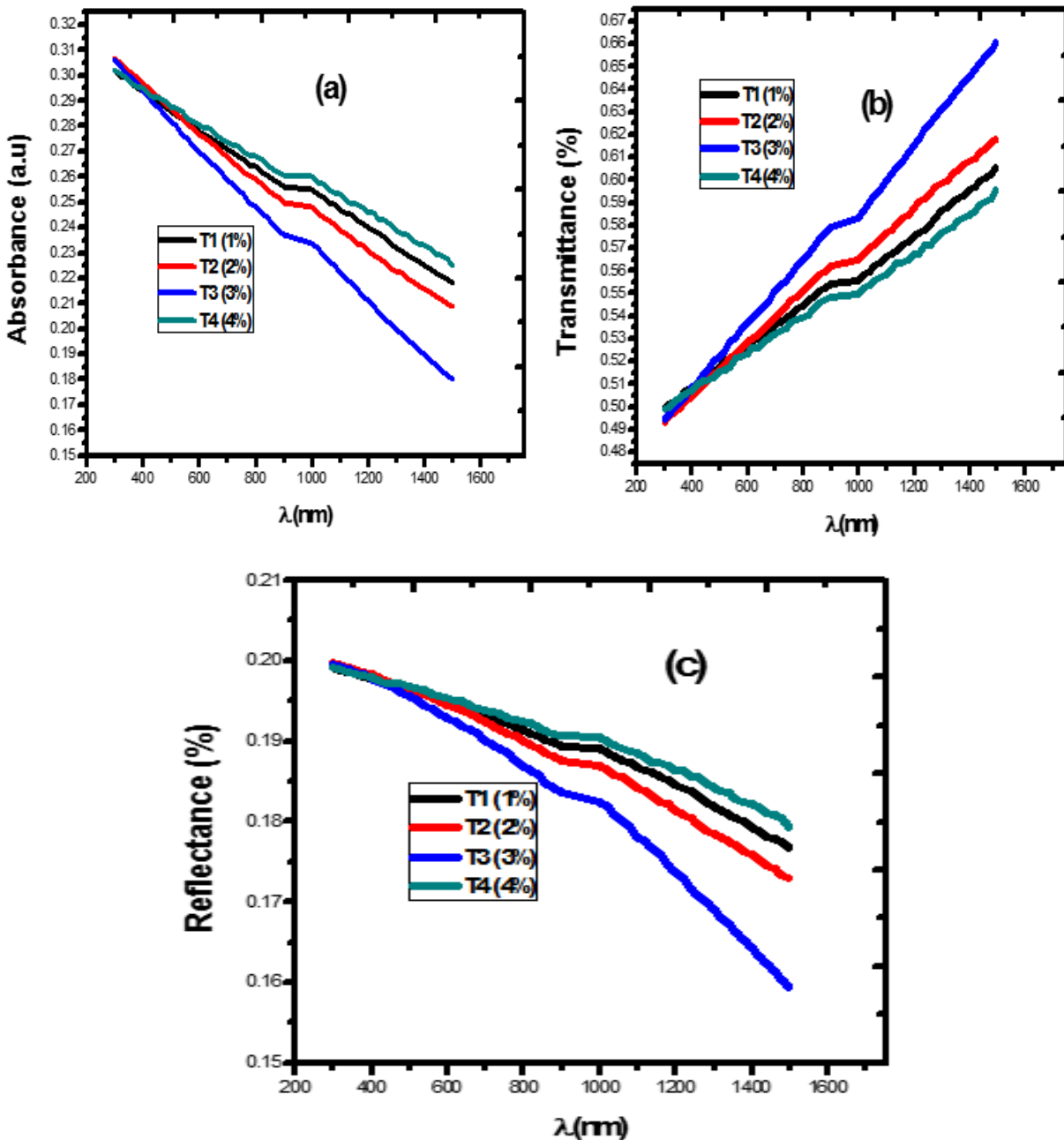

Figure 5. Plot of absorbance a), transmittance b) and reflectance c) against wavelength

The optical band gap energy of the SnZnSe thin films grown at varying dopant concentration of 1%, 2%, 3% and 4% is showed in Figure 6. From the plot sample T1, T2, T3 and T4 revealed the bandgap energy which was determine by extrapolating the straight part of the graph of absorption coefficient square against the photon energy to the photon energy axis. From the plot, bandgap energy is 2.0-2.3 eV [38, 39].
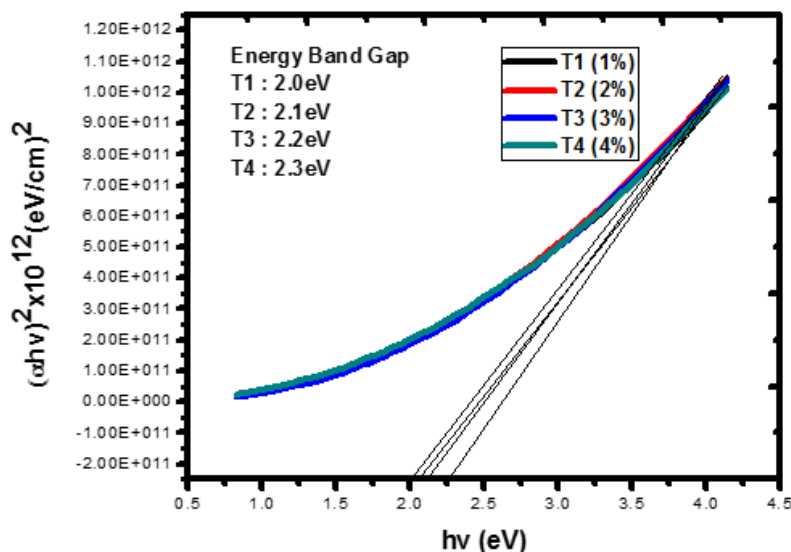

Figure 6. Plot of energy bandgap

The optical refractive index of the SnZnSe thin films in Figure 7**a** grown under the same parametric conditions and at varying dopant concentrations of 1%, 2%, 3% and 4% for sample T1, T2, T3, and T4 reveal that as the photon energy of the material increase the refractive index increases. It was observed that all the material grown at different dopant concentrations follow the same thread at the ultraviolet region which reveals the highest refractive index of SnZnSe thin films [38, 39]. SnZnSe cells grown will be a good material that will absorb energy from the sun and cells can also serve as a photovoltaic device and others application in the electronics industry. It was also noticed that SnZnSe can be used in the mass production of solar cells for the fabrication of lasting solar panels for alternative energy supply.

The extinction coefficient and optical conductivity of SnZnSe thin films in Figure 7**b** and **c** grown under the same parametric conditions and at varying dopant concentrations of 1%, 2%, 3% and 4% for sample T1, T2, T3, and T4 reveal that as the photon energy of the material increase the extinction coefficient and optical conductivity increases. It was observed that all the material grown at different dopant concentrations follow the same thread at the ultraviolet region which reveals the highest extinction coefficient and optical conductivity of SnZnSe thin films [33, 34]. SnZnSe cells grown will be a good material that will absorb energy from the sun and cells can also serve as a photovoltaic device and others application in the electronics industry. It was also noticed that SnZnSe can be used in the mass production of solar cells for the fabrication of lasting solar panels for alternative energy supply.
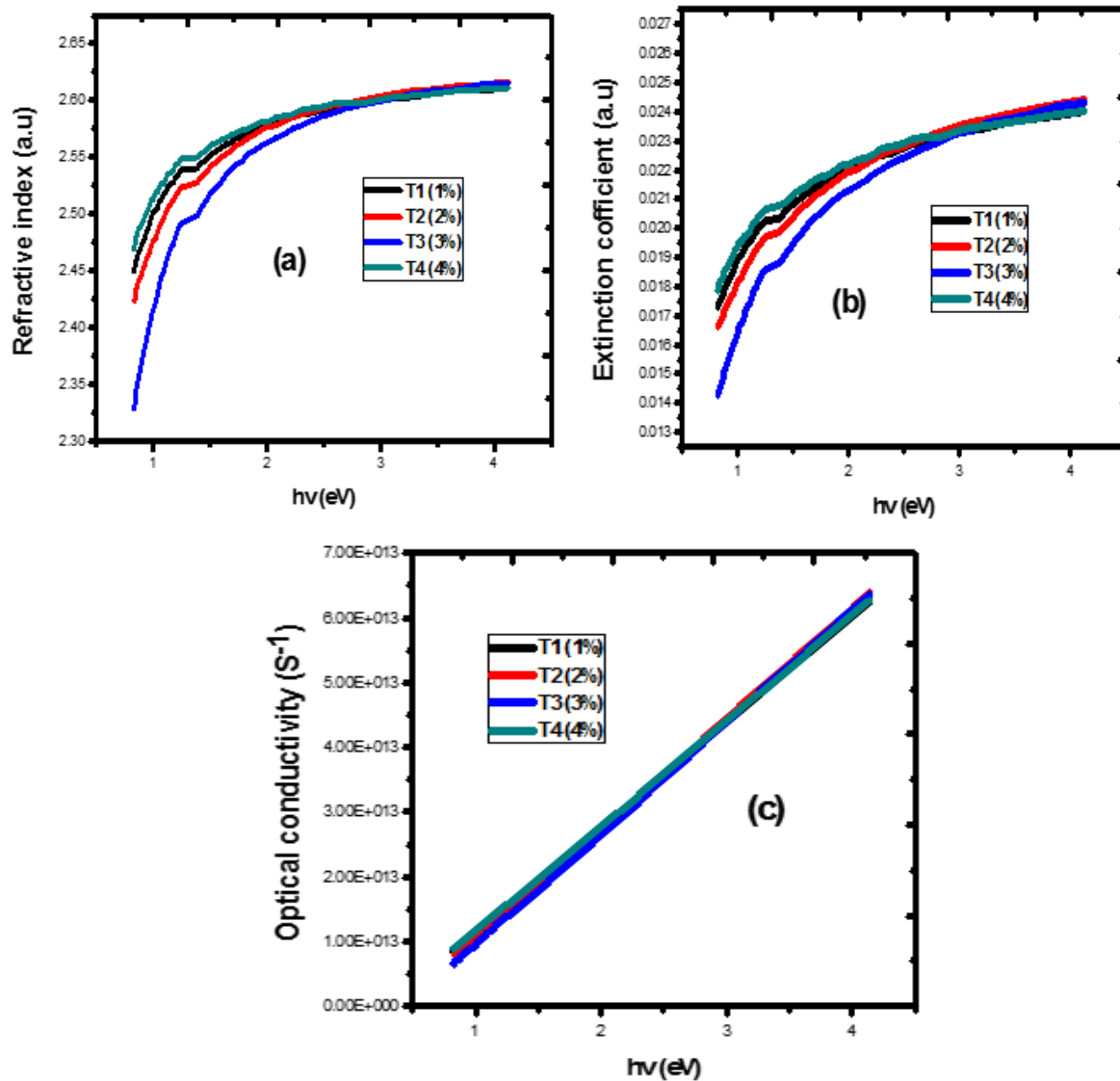
Figure 7. Plot of refractive index a), extinction coefficient b) and optical conductivity c) against photon Energy

The real and imaginary dielectric constant of SnZnSe thin films in Figure 8**a** and **b** grown under the same parametric conditions and at varying dopant concentration of 1%, 2%, 3% and 4% for sample T1, T2, T3 and T4 reveal that as the photon energy of the material increase the real and imaginary dielectric constant increases. It was observed that all the material grown at different dopant concentrations follow the same thread at the ultraviolet region which reveals the highest real and imaginary dielectric constant of SnZnSe thin films [38, 39]. SnZnSe cells grown will be a good material that will absorb energy from the sun and cells can also serve as a photovoltaic device and others application in the electronics industry. It was also noticed that SnZnSe can be used in the mass production of solar cells for the fabrication of lasting solar panels for alternative energy supply.
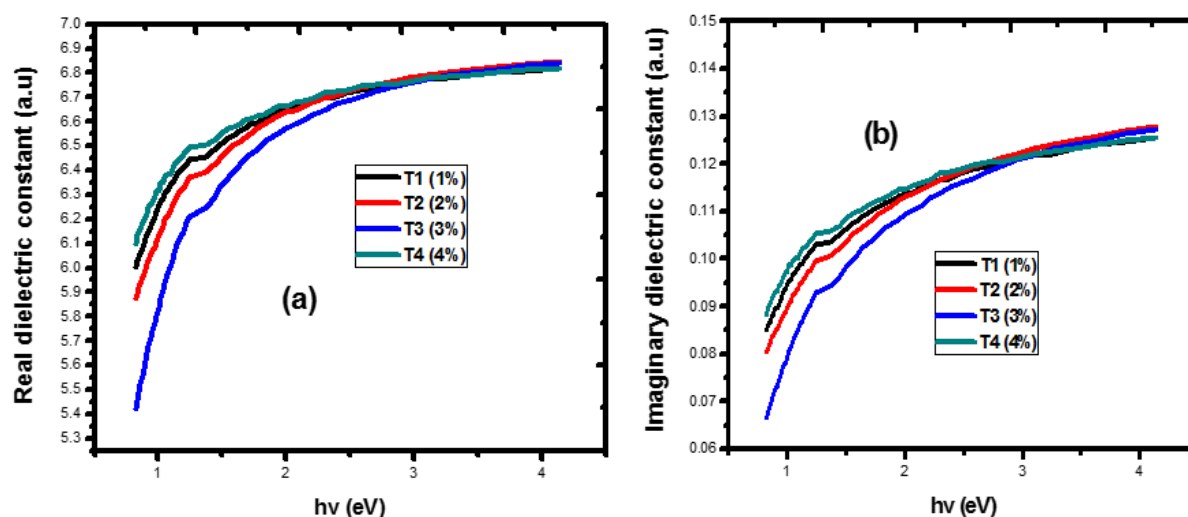
Figure 8. Plot of real dielectric constant a) and imaginary dielectric constant b) against photon energy

The electrical properties of SnZnSe thin films from Table 3, shown that the material deposited with 1%, 2%, 3%, and 4% dopant concentration shows increase in thickness from 202.33–248.49 nm with a corresponding decrease in the resistivity of the deposited material from 7.1234×10^3–4.3213×10^3 (Ω.cm) which result to the increase of the electrical conductivities of the deposited material. The high resistivity value makes this thin film useful in solar cells application to improve conversion efficiency as this could reduce the inevitable defects in solar cell fabrication during the actual production. As a result, SnZnSe thin films resistivity is quite suitable for a buffer layer in Solar cell, PV panel and photovoltaic devices [30, 31, 38, 39].

Table 3. Electrical properties of SnZnSe

Samples	Thickness, t (nm)	Resistivity, ρ (Ω.cm)	Conductivity, σ (Ωm/cm)$^{-1}$
T1 (1%)	202.33	7.1234×10^3	1.4038×10^{11}
T2 (2%)	232.24	6.3340×10^3	1.5787×10^{11}
T3 (3%)	238.42	5.2281×10^3	1.9127×10^{11}
T4 (4%)	248.49	4.3213×10^3	2.3141×10^{11}

Conclusions

The electrochemical deposition technique was successfully used to synthesize thin films of SnZnSe. The XRD of the films deposited on FTO substrates at different dopant concentration 1%, 2%, 3% and 4% shows the reflection peaks at (220), (221), (300), (310), (311), (222) and (320) with the lattice constant of a=7.189 Å. SEM revealed the random distribution of tiny nano-grains on the substrate, the nano-grains were observed to agglomerate due to the presence of large free energy characteristics of small particles. The optical bandgap of the deposited material increases from 2.0-2.3 eV as the dopant concentration increases. The optical absorbance spectra of SnZnSe thin films showed that the films grown under the same parametric conditions and at varying dopant concentration of 1%, 2%, 3% and 4% for sample T1, T2, T3, and T4 reveal that as the wavelength of the incident radiation increase the absorbance of

SnZnSe thin films decreases. The material grown at 1% and 4% has the same thread which reveals the lowest and the material is grown at 2% and 3% reveals highest which revealed that the SnZnSe cells grown will be a good material that will absorb energy from the sun and cells can also serve as a photovoltaic device and others application in the electronics industry. It was also noticed that SnZnSe can be used in the mass production of solar cells for the fabrication of lasting solar panels for alternative energy supply.

Acknowledgements

Disclosure Statement

No potential conflict of interest was reported by the authors.

Orcid

Imosobomeh Lucky Ikhioya iD 0000-0002-5959-4427

References

[1]. Young H.D., Freedman R.A. *Addison Wesley*., 2008, **I**:232

[2]. Wei A., Zhao X., Liu J., Zhao Y. *Physica B*., 2013, **410**:120

[3]. Venkatachalam S., Jeyachandran Y.L., Sureshkumar P., Dhayalraj A., Mangalaraj D., Narayandass Sa.K., Velumani S. *Materials Characterization*, 2007, **58**:794

[4]. Xu J., Wang W., Zhang X., Chang X., Shi Z., Haarberg G.M. *J. Alloys Compd*., 2015, **632**:778

[5]. Agawane G.L., Seung W.S., Suryawanshia M.P., Gurav K.V., Moholkara A.V., Leeb J.Y., Patil P.S., Jae H.Y., Jin H.K. *Ceramics International*, 2013, **06**:011

[6]. Bakiyaraj G., Dhanasekaran R. *Appl. Nanosci*., 2013, **3**:125

[7]. Deshmukh L.P., Pingale P.C., Kamble S.S., Mane S.T., Pirgonde B.R., Sharonb M., Sharon M. *Mater. Lett*., 2013, **92**:308

[8]. Chandramohan R., Mahalingam T., Chu J.P., Sebastian P.J. *Journal of New Material for Electrochemical Systems*, 2005, **8**:143

[9]. Akhtar M.S., Malik M.A., Riaz S., Naseem S., O'Brien P. *Mater. Sci. Semicond. Process*., 2015, **30**:292

[10]. Dhanasekaran V., Mahalingam T., Rhee J., Chu J.P. *Optik*, **124**:255

[11]. Lohar G.M., Shinde S.K., Rath M.C., Fulari V. J. *Mater. Sci. Semicond. Process*., 2014, **26**:548

[12]. Mehta C., Saini G.S.S., Abbas J.M., Tripathi S. K. *Appl. Surf. Sci*., 2009, **256**:608–614

[13]. Mahalingam T., Kathalingam A., Lee S., Moon S., Kim D.Y. *Journal of New Material for Electrochemical Systems*, 2007, **10**:15-19

[14]. Pardo A.P., Gonzalez H.G., Castro-Lora López-Carreño L.D., Martínez H.M., Salcedo N.J. T. *J. Phys. Chem. Solid*., 2014, **75**:713

[15]. Mahalingam T., Kathalingam A., Lee S., Moon S., Kim Y.D. *J. New Mater. Electrochemi. Sys*., 2007, **10**:15

[16]. Imran M., Abida S., Nawazish A.K., A.A. Khurram, Nasir M. *Thin Solid Film*., 2018, **11**:1

[17]. Pentia E., Draghici V., Sarua G., Mereu B., Pintilie L., Sava F., Popescu M. *J. Electrochem. Soc*., 2004, **151**:729

[18]. Rajesh Kumar T., Prabukanthan, Harichandran G., Theerthagiri J., Chandrasekaran S, Madhava J. *Ionics*, 2017, **23**:2497

[19]. Rajesh T.K., Prabukanthan P., Harichandran G., Theerthagiri J., Tetiana T.,

Gilberto M., Bououdina M. *Journal of Solid State Electrochemistry*, 2017, **27**:254

[20]. Sadekar H.K., Ghule A.V., Sharma R. *Composite Part B.*, 2013, **44**:553

[21]. Samantilleke A.P., Boyle M.H., Young J., Dharmadas I.M., *Journal of Materials Science: Materials in Electronics*, 1998, **9**:231

[22]. Ahna K., Jeon J.H., Jeong S.Y., Kim J.M., Ahn H.S., Kim J.P., Jeong E.D., Cho C.R. *Current Applied Physics.*, 2012, **12**:1465

[23]. Hwang D.H., Ahn J.H., Hui K.N., Hui K.S., Son Y.G. *Nanoscale Research Letters*, 2012, **7**:1

[24]. Bosco J.P., Demers S.B., Kimball G.M., Lewis N.S., Atwater H.A. *Journal of Applied Physics.*, 2012, **112**:093703

[25]. Yano S., Schroeder R., Sakai H., Ullrich B. *Applied Physics Letters.*, 2003, **82**:2026

[26]. Huang M.W., Cheng Y.W., Pan K.Y., Chang C.C., Shieu F.S., Shih H.C. *Applied Surface Science.*, 2012, **261**:665

[27]. Xu G., Ji S., Miao C., Liu G., Ye C. *Journal of Materials Chemistry*, 2012, **22**:4890

[28]. Nagamani K., Revathi N., Prathap P., Lingappa Y., Reddy K.T.R. *Current Applied Physics.*, 2012, **12**:380

[29]. Agawane G.L., Wook Shin S., Sung Kim M., Suryawanshi M.P., Gurav K.V., Moholkar A.V., Yong Lee J., Yun J.H., Patil P.S., Hyeok Kim J. *Current Applied Physics.*, 2013, **13**:850

[30]. Ikhioya I.L., Ekpunobi A.J. *Journal of Nigeria Association of Mathematical Physics*, 2014, **28**:281

[31]. Ikhioya I.L., Ekpunobi A.J. *Journal of Nigeria Association of Mathematical Physics.*, 2015, **29**:325

[32]. Harbeke G. *North-holland Pub. Co. Amsterdam*, 1972, 234

[33]. Ikhioya I.L., Okoli D.N., Ekpunobi A.J. *SSRG International Journal of Applied Physics*, 2019, **6**:55

[34]. Ikhioya I.L., Okoli D.N., Ekpunobi A.J. *International Journal of ChemTech Research,* 2019, **12**:200

[35]. Sajjadnejad M., Karimi Abadehb H. *Section A: Theoretical, Engineering and Applied Chemistry*, 2020, **4**:422

[36]. Miranzadeh M., Afshari F., Khataei B., Kassaee M. *Advanced Journal of Chemistry, Section A: Theoretical, Engineering and Applied Chemistry*, 2020, **4**:In press

[37]. Magu T., Agobi A., Hitler L., Dass P. *Journal of Chemical Reviews*, 2019, **1**:19

[38]. Ikhioya I.L., Okoli D.N., Ekpunobi A.J. *International Journal of ChemTech Research*, 2019, **12**:200

[39]. Ikhioya I.L., Okoli D.N, Ekpunobi A.J. *International Journal of Applied Physics,* 2019, **6**:55